# A statistical study of plasmaspheric plumes and ionospheric outflows observed at the dayside magnetopause

S. H. Lee, H. Zhang, Q. -G. Zong, A. Otto, H. Rème, E. Liebert

AGU PUBLICATIONS

JGR

Journal of Geophysical Research: Space Physics

RESEARCH ARTICLE

10.1002/2015JA021540

**Key Points:**
- Statistical study for plumes and ionospheric outflows observed by Cluster near the magnetopause
- Plumes (outflows) tend to occur during southward (northward) IMF and moderate geomagnetic activity
- Enhanced occurrence rates of outflows were observed in the dawnside (duskside) for IMF By > 0 (By < 0)

**Correspondence to:**
H. Zhang,
hzhang14@alaska.edu

**Citation:**
Lee, S. H., H. Zhang, Q.-G. Zong, A. Otto, H. Rème, and E. Liebert (2016), A statistical study of plasmaspheric plumes and ionospheric outflows observed at the dayside magnetopause, *J. Geophys. Res. Space Physics*, *121*, 492–506, doi:10.1002/2015JA021540.

Received 4 JUN 2015
Accepted 4 JAN 2016
Accepted article online 11 JAN 2016
Published online 30 JAN 2016



# A statistical study of plasmaspheric plumes and ionospheric outflows observed at the dayside magnetopause

**S. H. Lee[1,2], H. Zhang[1], Q.-G. Zong[3], A. Otto[1], H. Rème[4,5], and E. Liebert[6]**

[1]Geophysical Institute, University of Alaska Fairbanks, Fairbanks, Alaska, USA, [2]Now at NASA Goddard Space Flight Center, Greenbelt, Maryland, USA, [3]Institute of Space Physics and Applied Technology School of Earth and Space Sciences, Peking University, Beijing, China, [4]University of Toulouse, UPS-OMP, IRAP, Toulouse, France, [5]CNRS, IRAP, Toulouse, France, [6]Institute for Geophysics and Extraterrestrial Physics, Braunschweig, Germany

**Abstract** We present a statistical study of plasmaspheric plumes and ionospheric outflows observed by the Cluster spacecraft near the dayside magnetopause. Plasmaspheric plumes are identified when the low-energy ions (<1 keV) with ~90° pitch angle distributions are observed by the Cluster Ion Spectrometer/Hot Ion Analyzer instrument. The ionospheric outflows are characterized by unidirectional or bidirectional field-aligned pitch angle distributions of low-energy ions observed in the dayside magnetosphere. Forty-three (10%) plasmaspheric plume events and 32 (7%) ionospheric outflow events were detected out of the 442 times that C3 crossed the dayside magnetopause between 2007 and 2009. The occurrence rate of plumes at duskside is significantly higher than that at dawnside. The occurrence rate of outflows shows a weak dawn-dusk asymmetry. We investigate the dependence of the occurrence rates of plumes and ionospheric outflows on geomagnetic activity and on solar wind/interplanetary magnetic field (IMF) conditions. The plume events tend to occur during southward IMF (duskward solar wind electric field) and moderate geomagnetic activity ($Kp = 3$, $-30 \leq Dst < -10$ nT). However, the ionospheric outflow events tend to occur during northward IMF (dawnward solar wind electric field). The ionospheric outflows do not occur when $Kp = 0$, and the occurrence rate of the ionospheric outflows does not have a clear *Dst* dependence. Seventy-five percent (46%) of the outflows are observed in the duskside for negative (positive) IMF $B_y$. Conversely, 54% (25%) of the outflows are observed in the dawnside for positive (negative) IMF $B_y$. Finally, the occurrence rates of both plumes and outflows increase with solar wind dynamic pressure.

## 1. Introduction

There are two types of low-energy plasma populations that can dominate the dayside magnetosphere: plasma of plasmaspheric origin (plasmaspheric wind, blob, and plume) and of ionospheric origin (ionospheric outflow and warm plasma cloak). The low-energy, dense plasma of these two origins supplies particles to the cavity of the magnetosphere and can extend to a distance near the magnetopause. Figure 1 shows a sketch of several low-energy plasma populations that can be observed near the dayside magnetopause.

The plasmaspheric plasma can expand beyond the plasmapause in the form of the blobs, the plume, and the plasmaspheric wind. The drainage plume is the extension of the outer region of the plasmasphere [*Chen and Wolf*, 1972; *Lemaire*, 2000; *Green et al.*, 2002; *O'Brien and Moldwin*, 2003]. When the interplanetary magnetic field (IMF) turns southward, the plasmapause that is formed by the combination of the corotational and solar wind-driven convection electric fields moves inward across the nightside and a sunward bulge develops near the duskside. Since southward IMF enhances the sunward convection across the dayside magnetosphere, a distinct plasmaspheric plume can be formed at the duskside [*Goldstein et al.*, 2003]. The blobs are formed when the plasmaspheric plasma is detached from the plasmasphere [*Chappell*, 1974]. *Goldstein et al.* [2004] suggested that a blob of plasmaspheric plasma could be formed when the plume moves outward and becomes isolated. The plasmaspheric wind continuously releases plasmaspheric plasma into the magnetosphere across the geomagnetic field lines during quiet and moderately active geomagnetic conditions ($Kp < 3$) [*Dandouras*, 2013].

There are four possible source regions for the ionospheric outflow as classified by location and energy distribution function: the auroral region, the cleft ion fountain, and the polar wind. The ionospheric ions can be accelerated by the ambipolar electric field arising from a pressure gradient of thermal electrons or by the electric

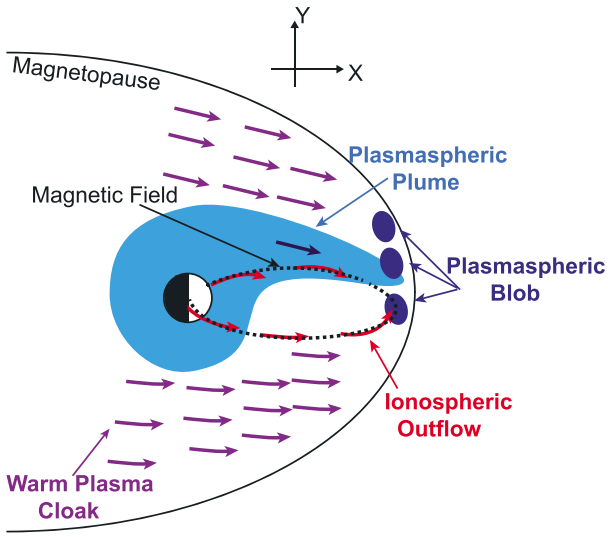


**Figure 1.** A sketch of the major low-energy ion populations that can be observed in the dayside magnetosphere.

field caused by the spatial separation between the electrons and heavy ions, resulting in the light ions escaping from the polar ionosphere. This is one possible mechanism that can generate the ionospheric ion outflow from the polar cap regions [*Yau and André*, 1997; *Yau et al.*, 2007]. There are two types of plasma of ionospheric origin: the ionospheric outflow and the warm plasma cloak. The ionospheric outflow is directly coming from one or both hemispheres. The warm plasma cloak is formed when the ionospheric outflow is transported toward the nightside and then brought back to the dayside magnetosphere by $\mathbf{E} \times \mathbf{B}$ convection. The warm plasma cloak has an intermediate energy (a few eV to hundreds of eV), which is greater than the energy of a direct upward outflow and lower than that of the populations in the plasma sheet or ring current [*Chappell et al.*, 2008]. Both the ionospheric outflow and the warm plasma cloak have unidirectional or bidirectional field-aligned ion pitch angle distributions.

Plasmaspheric plumes have been identified using several methods. Plumes were identified when their densities exceeded the model values at different *L* shells obtained from the empirical model of *Sheeley et al.* [2001] using the CRRES data set at geosynchronous orbit [*Moldwin et al.*, 2004] and using the Time History of Events and Macroscale Interactions during Substorms (THEMIS) measurements at the dayside magnetopause [*Walsh et al.*, 2013]. *Chen and Moore* [2006] used measurements from the Thermal Ion Dynamics Experiment on the Polar spacecraft (TIDE/Polar) orbiting in the dayside outer magnetosphere beyond geosynchronous distances to identify the plasmaspheric drainage plume. They defined plasmaspheric plumes when their peak energy is above the spacecraft potential (a few eV) and below the upper energy limit of the instrument (~400 eV), and when the flow is perpendicular to the magnetic field. *Darrouzet et al.* [2008] identified plumes from a significant and localized density increase (10 $cm^{-3}$ minimum) in the electron density profile. *André and Cully* [2012] also identified the plasmaspheric drainage region where high-density (up to a few tens of $cm^{-3}$) low-energy ions were observed during Cluster spacecraft crossings of the magnetopause.

Ionospheric outflows have also been observed by several satellites [*Yau et al.*, 1986; *Peterson et al.*, 2001; *Cully et al.*, 2003; *Andersson et al.*, 2005; *Redmon et al.*, 2012]. *Peterson et al.* [2006] identified that the ionospheric outflows when the peak fluxes were greater than $10^{10}$ ions/$m^2$ s sr and their ion distributions had less than 90° pitch angle distributions that were observed from the Southern Hemisphere. The data were recorded by the Toroidal Ion Mass-Angle Spectrograph instrument on the Polar satellite with a mean altitude of about 7500 km during solar minimum. The ionospheric outflows can be classified in terms of their pitch angle distributions: beam, conic, and upflowing ions (UFI) [*Peterson et al.*, 2006]. An ion beam is defined as an ion distribution which has a peak flux along the upward direction of the local magnetic field (from 0° to 30° pitch angle distributions), and an ion conic has pitch angles with peaks in the range of 30° to 75°. A UFI is defined as the combination of beams and conics so that it has a peak flux in the range of 0° to 75° pitch angle distributions. The warm plasma cloak has been observed in the dayside magnetosphere by the ATS, ISEE, SCATHA, DE, and Polar satellites [*Lennartsson and Reasoner*, 1978; *Baugher et al.*, 1980; *Fennell et al.*, 1981; *Kaye et al.*, 1981; *Nagai et al.*, 1983; *Sagawa et al.*, 1987; *Giles et al.*, 1994; *Chappell et al.*, 2008].

Density ranges for both plasmaspheric plumes and ionospheric outflows, their spatial distribution, and the dependence of their occurrence rates on the geomagnetic activity and solar wind/IMF conditions have been studied. Density of plumes varies from a few $cm^{-3}$ to a few hundred $cm^{-3}$, depending on their locations (*L* shell and latitude) [*Chappell*, 1972; *Sauvaud et al.*, 2001; *Walsh et al.*, 2013]. *Chen and Moore* [2006] found that significantly more plasmaspheric plume events, observed by TIDE/Polar near polar apogee (>5 $R_E$), occurred at the duskside than at the dawnside. *Darrouzet et al.* [2008] showed that the plasmaspheric plume events were observed mostly for moderate *Kp* (= 3–6) and not for small *Dst*.

The density of the warm plasma cloak ions ranges from 0.5 to 3 $cm^{-3}$, as observed by TIDE near Polar apogee [*Sagawa et al.*, 1987; *Chappell et al.*, 2008]. These ions are found more often at dawnside than duskside. *Nagai et al.* [1983] found that the occurrence rate of the ionospheric outflows (<100 eV), measured by the Plasma Composition Experiment on board ISEE in the range of $L = 3–10$, increased with decreasing *Kp*. *Cully et al.* [2003] showed that the ionospheric outflow rates were strongly correlated with the solar wind dynamic pressure, the solar wind electric field, and variation in the IMF.

Observations of plasmaspheric plumes and ionospheric outflows at different locations in the magnetosphere have been made using various spacecraft [e.g., *Chen and Moore*, 2006; *Chappell et al.*, 2008; *Walsh et al.*, 2013]. However, no study has been conducted on the characteristics of both plumes and ionospheric outflows near the magnetopause. These low-energy ions can play an important role in magnetospheric dynamics, such as in magnetic reconnection. Several analytic and numerical studies have predicted that high-density plasma on the magnetospheric side, such as the plasmaspheric plume and ionospheric outflow, decreases the Alfvén speed and slows down the reconnection process at the magnetopause as the reconnection rate scales with the Alfvén speed [*Shay and Swisdak*, 2004; *Borovsky et al.*, 2008, 2013]. *Walsh et al.* [2013] showed that reconnection jet velocities are on average slower when a cold dense plume is present at the dayside reconnection region based on THEMIS observations. *Lee et al.* [2014] suggested that the plasmaspheric ions could weakly participate in reconnection when they enter at high latitudes in the reconnection region, and *Wang et al.* [2014] also concluded that the dynamics of the cold dense ions in reconnection differ depending on which region of the reconnection (close to or farther away from the diffusion region) they entered. Studying the characteristics and tendencies of the cold dense plasma near the dayside magnetopause is necessary for an in-depth understanding of the effect of the cold dense plasma on reconnection and for developing a global picture of the solar wind-magnetosphere-ionosphere coupling.

In this paper, we use Cluster in situ measurements to identify low-energy ions of ionospheric origin (called "ionospheric outflow" in this paper) and plasmaspheric origin (called "plasmaspheric plume" in this paper) observed near the dayside magnetopause. We analyze their densities, spatial distributions, and occurrence rates to determine the underlying dependence on solar wind/IMF conditions and geomagnetic activity.

## 2. Methodology

### 2.1. Instrumentation and Data

This study uses C3 measurements from 18 months of intermittent observation (from January to May and December) from 2007 to 2009. From these 3 years, we have identified 43 (10%) plasmaspheric plume events and 32 (7%) ionospheric outflow events that occurred when Cluster crossed the dayside magnetopause (442 total magnetopause crossings). The trajectories of Cluster were evenly distributed between dawnside and duskside. However, Cluster spent more time and covered different absolute latitudes in the Southern Hemisphere compared to the Northern Hemisphere, and this asymmetry in trajectories makes it difficult to make an accurate comparison between the two hemispheres. Low-energy ions (either plumes or outflows) were detected in 15% (68 of 442) of all dayside magnetopause crossings (both plume and ionospheric outflow were observed for seven magnetopause crossings).

We use plasma data from the Hot Ion Analyzer (HIA) sensor of the Cluster Ion Spectrometer (CIS) instrument [*Rème et al.*, 2001], the spacecraft potential from the Electric Field and Wave (EFW) instrument [*Gustafsson et al.*, 2001], and the magnetic field data measured by the fluxgate magnetometer [*Balogh et al.*, 2001] on board the Cluster spacecraft [*Escoubet et al.*, 1997, 2001]. The CIS/HIA ion detector provides the 3-D velocity distribution with high-energy resolution, covering the energy range from about 5 eV to 32 keV with high angular resolution. The HIA sensor provides a 360° instantaneous field of view, which is divided into angle sections. The electron density ($N_e$) can be estimated using the spacecraft potential, which is the potential difference between the antenna probes and the spacecraft body measured by the EFW experiment [*Pedersen*

*et al.*, 2008]. The spacecraft potential covers a large density range from about $10^{-3}$ cm$^{-3}$ to approximately $10^{2}$ cm$^{-3}$ with high time resolution, ~0.1 s [*Gustafsson et al.*, 2001]. Since the CIS/HIA detector has a limit for measuring the lower energy (<5 eV) ions, the electron density derived through the spacecraft potential must be used to take into account the density of the lower energy (<5 eV) ions.

### 2.2. Identifications of the Plume and Ionospheric Outflow Events

The events were selected on the basis of two criteria. (1) We only selected events when the low-energy ion particle energy flux was greater than $10^{5}$ keV/(cm$^{2}$ s sr keV), which was chosen as a lower limit for the energy flux of low-energy ions to be comparable with the particle energy fluxes of the magnetospheric ions. Events were manually identified by requiring the cold ions to be clearly visible in the ion energy spectrum from the CIS/HIA instrument. To be detected, the energy of the cold ions must be larger than the threshold of the CIS/HIA instrument (5 eV). (2) The cold ions were present for longer than 2 min.

Plasmaspheric plumes can be distinguished from the ionospheric outflows by using the ion pitch angle distribution. The plasmaspheric plume ions have ~90° pitch angle distributions (perpendicular to the magnetic field). The plume is formed when the strength of the convection electric field suddenly increases. Increasing convection causes the duskside bulge of the plasmasphere along the open-drift paths [*Goldstein et al.*, 2005]. Thus, a large amount of cold ions drift to the dayside magnetopause. The drift associated with the enhanced convection electric field is perpendicular to the magnetic field. In contrast, the pitch angle distributions for the ionospheric outflows from one or both hemispheres are mostly 0° and/or 180° peaked (unidirectional or bidirectional pitch angle distributions); i.e., the ionospheric outflows are field-aligned flows [*Horwitz et al.*, 1982; *Chappell et al.*, 2008].

Figure 2 presents examples of a plume case (left) and an ionospheric outflow case (right) from 03:00 to 05:00 UT on 10 February 2007 and from 05:00 to 07:00 UT on 6 March 2008, respectively. The C3 satellite was located at $(X, Y, Z)_{GSM} = (9.86, 6.10, 4.75)\,R_E$ for the plume event at 03:00 UT and $(X, Y, Z)_{GSM} = (10.27, 2.94, 2.70)\,R_E$ for the ionospheric outflow event at 05:00 UT. From Figures 2a to 2f, the ion energy spectrum, the ion (<1 keV) pitch angle distribution, ion density, electron density derived from the spacecraft potential, the ion velocity moments $V_x$ (blue), $V_y$ (green), and $V_z$ (red) (km/s), and the three magnetic field components $B_x$ (blue), $B_y$ (green), and $B_z$ (red) (nT) in geocentric solar magnetospheric (GSM) coordinates are shown for the 2 h time intervals. The ion moments (the ion number density and velocity) are calculated for ions in the range of ~5 eV/$e$–32 keV/$e$ measured by the HIA instrument (without mass discrimination).

Figure 2a shows the ion energy flux from HIA. The low-energy ion flux is irregularly shown in the ion energy-time spectrogram for the plume event from 03:00 UT to 03:50 UT (Figure 2a). The localized low-energy ion flux can be due to the lumpiness (density variations) of the plume plasma or to plasmaspheric plumes consisting of isolated plasmaspheric filaments or blobs [*Borovsky et al.*, 2008; *Murakami et al.*, 2013].

Ion dispersions with multiple energies are seen from 05:10 UT to 06:30 UT in the ion energy spectrum for the ionospheric outflow event (Figure 2a). The energy dispersion signature is possibly due to the time-of-flight effect when the ionospheric ions stream away from the hemispheres along closed magnetic field lines.

Figure 2b shows that the plume has a ~90° pitch angle distribution and the ionospheric outflow has a bidirectional field-aligned pitch angle distribution. The average ion densities are 0.8 cm$^{-3}$ for plumes and 0.4 cm$^{-3}$ for ionospheric outflows (Figure 2c). There are large ion density variations in the plume event. The average electron densities are 5.0 cm$^{-3}$ for plumes and 4.1 cm$^{-3}$ for the ionospheric outflows (Figure 2d). The ion densities are lower than the electron densities because the cold ions with energy lower than 5 eV (threshold of HIA) cannot be detected by the instrument. The ion and electron densities for plumes are higher than those for the ionospheric outflows.

Figure 2e shows three components of ion bulk velocity. The accelerated plasma flows $V_z$ (~300 km/s) and $V_y$ (~200 km/s) were observed in the boundary layer for the plume and ionospheric outflow events, respectively. The high-speed flows in the boundary layer accompanied by changes in the magnetic field direction are typical signatures of magnetic reconnection. For the plume event, the average IMF $B_z$ was −1.7 nT (southward IMF condition), which was obtained from the 5 min averaged OMNI data set available at OMNIWeb, and the $z$ component of the magnetic field changed from positive (~30 nT) to negative (~−20 nT) when the high-speed flows ($V_z$) were observed. The accelerated ion jet $V_z$ switched direction at 04:05 UT, indicating that C3 crossed the reconnection site to the other side of the X line. For the ionospheric outflow event, the average IMF $B_z$ and

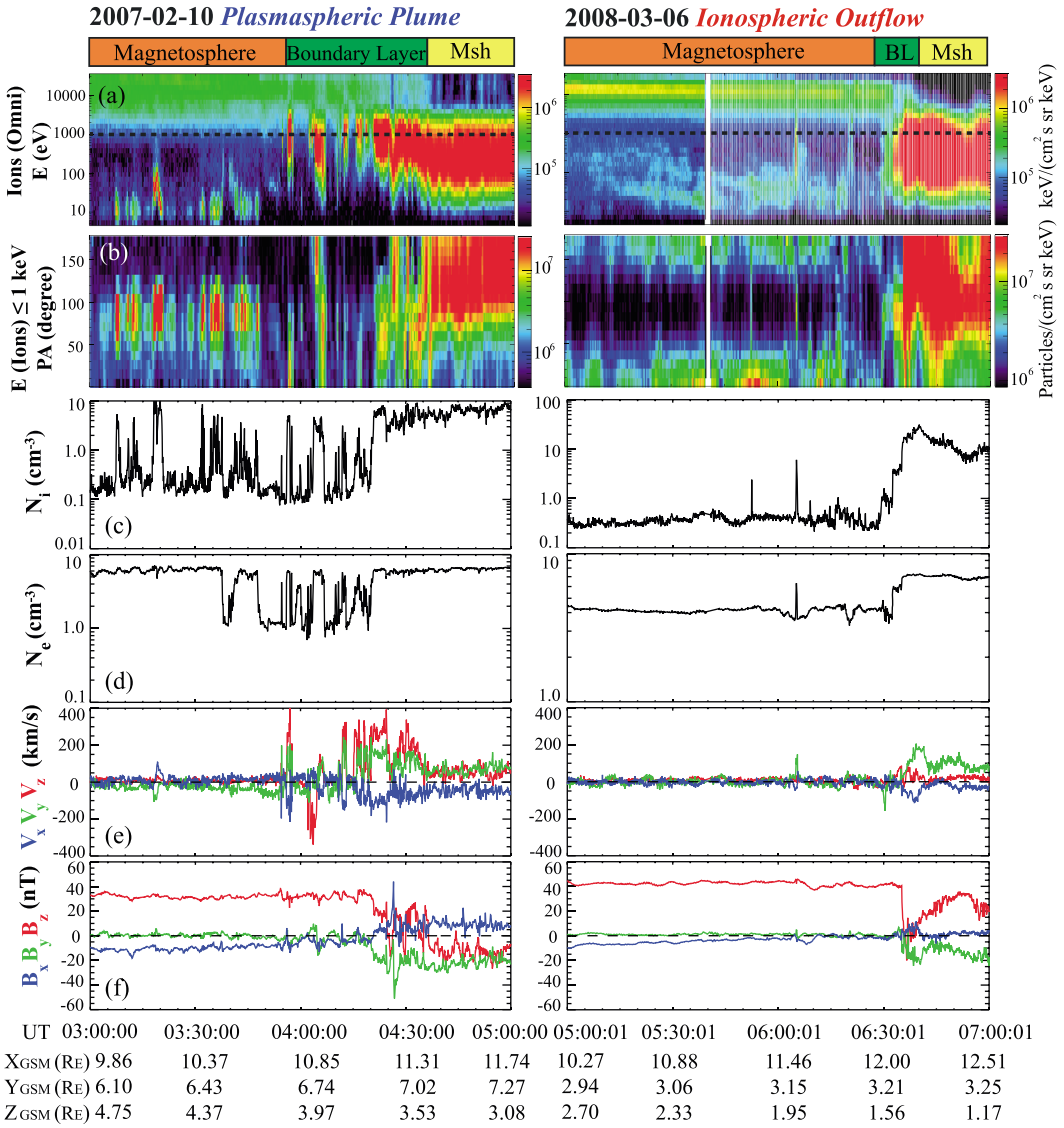


**Figure 2.** Examples of (left) a plume case and (right) an ionospheric outflow case near the dayside magnetopause observed by C3. (a) HIA omnidirectional energy-time spectrogram in energy flux units (no mass discrimination), (b) the pitch angle distribution for low-energy ions (<1 keV), (c) ion density, (d) electron density from the spacecraft potential, and (e) the three velocity and (f) magnetic field components in GSM coordinates, respectively.

$B_y$ were 0.9 nT (northward IMF condition) and −1.0 nT, respectively. The *y* component of the magnetic field changed from positive (~5 nT) to negative (~−20 nT) when the high-speed flow jet ($V_y$) occurred.

In the following section, we statistically examine the occurrence rate of plasmaspheric plumes and ionospheric outflows and their dependence on geomagnetic activity and on solar wind/IMF conditions. We also compare the characteristics of plasmaspheric plumes and ionospheric outflows.

## 3. Results

### 3.1. Occurrence Rate of Plasmaspheric Plumes and Ionospheric Outflows

Figure 3 shows the trajectories (gray lines) of Cluster and the distribution of plasmaspheric plumes (blue) and ionospheric outflows (red) in GSM coordinates. The occurrence rates of plumes (10%) and ionospheric outflows (7%) are less than those from other statistical studies. *Walsh et al.* [2013] showed that the occurrence rate of plumes at the dayside magnetopause was 12.5% based on THEMIS observations, and *Darrouzet et al.* [2008] showed that the occurrence rate of plasmaspheric plumes observed by Cluster at 4–11 $R_E$ was 15%. Plasmaspheric-like plasma was present outside the plasmapause during 30% (169 of the 558 plasmapause

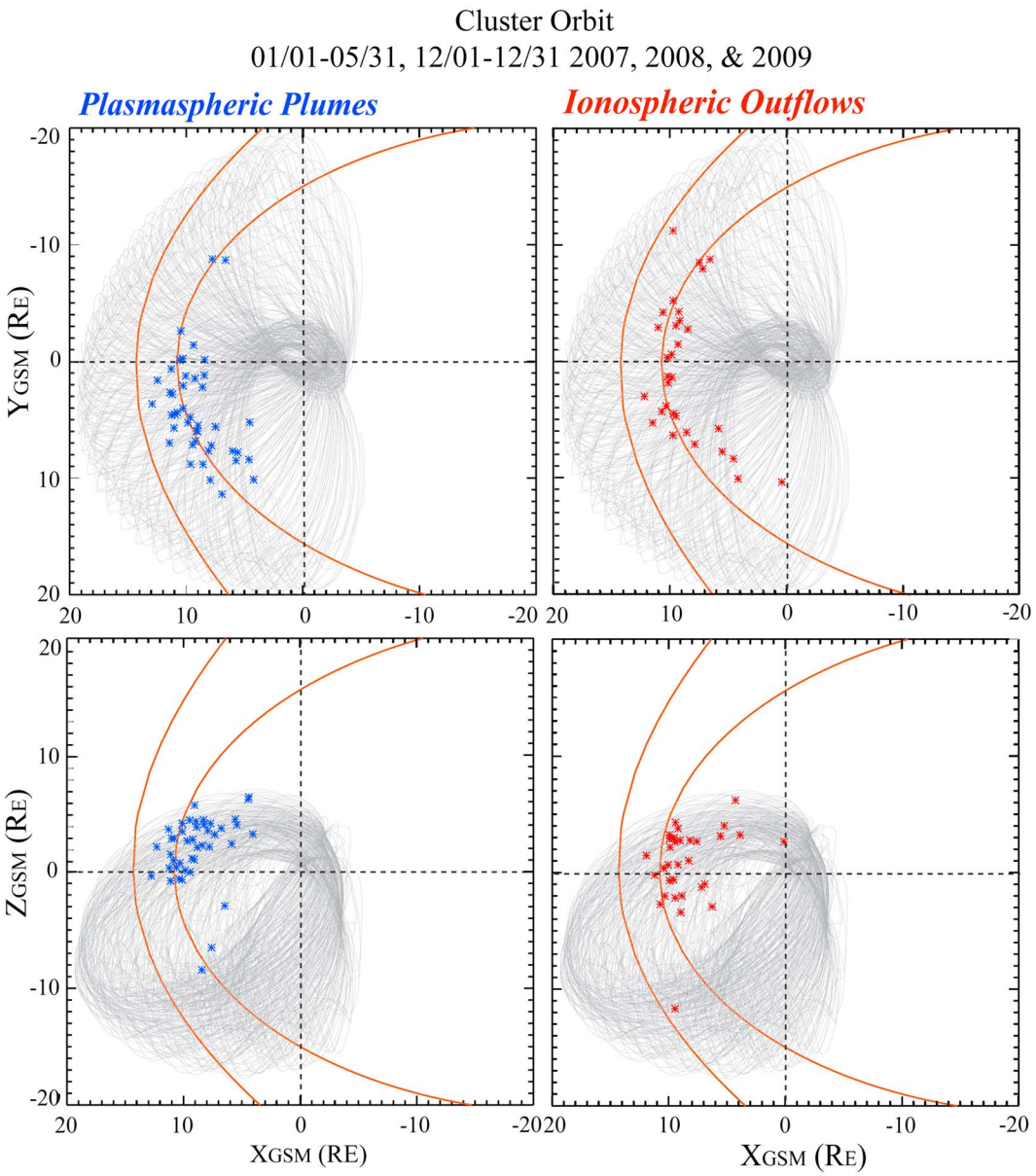


**Figure 3.** Distributions of plasmaspheric plumes (blue) and ionospheric outflows (red) as detected by Cluster 3 while crosses the dayside magnetopause. The gray lines show the traces of Cluster spacecraft from 1 January to 31 May and December 2007, 2008, and 2009 in the GSM coordinate system *X*-*Y* and *X*-*Z* planes. The red lines represent the bow shock (outer) and the magnetopause (inner), which are determined by the Fairfield model.

crossings) of the plasmapause crossings by CRRES [*Moldwin et al.*, 2004]. *André and Cully* [2012] showed that the ionospheric outflow of low-energy ions can dominate 50–70% of the time on the dayside magnetosphere. In our study, plasmaspheric plumes and ionospheric outflows were identified in the CIS/HIA data, which may lead to lower occurrence rates of the low-energy ions since cold ions with energy lower than the threshold (5 eV) of the detector cannot be detected.

Of the plasmaspheric plumes (43) and ionospheric outflows (32) identified, both plasmaspheric plumes and ionospheric outflows were observed during seven magnetopause crossings so that the low-energy ion events (either plumes or outflows) were detected in ~15% (68 of 442) of dayside magnetopause crossings. Seventy-six percent (57 of 75) of the low-energy ion events were observed in the duskside, even though the Cluster orbits were evenly distributed between dawnside and duskside. Ninety-one percent of the plume events were detected in the duskside, while only 9% were observed in the dawnside. This is consistent with

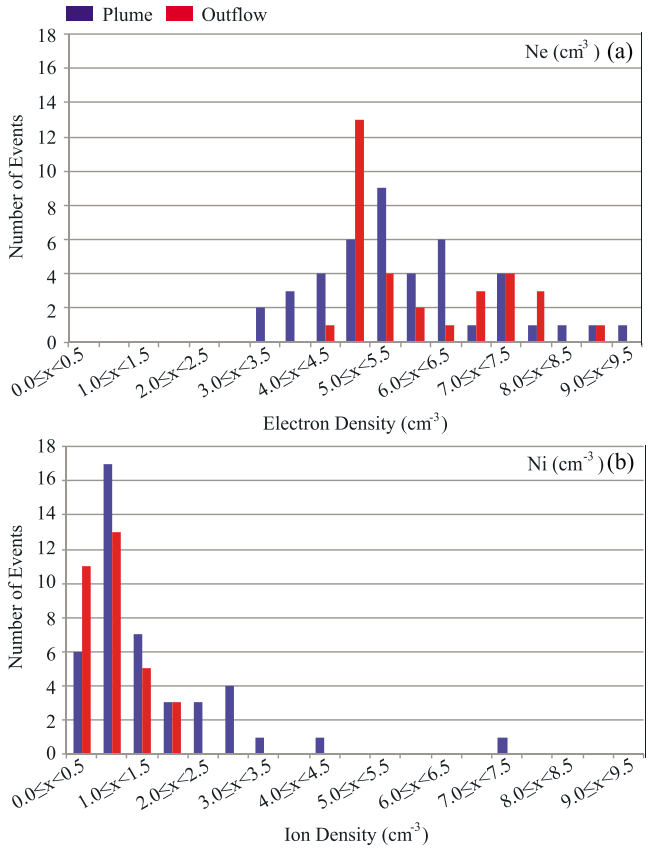


**Figure 4.** Distributions of plume and ionospheric outflow events as a function of (a) electron density and (b) ion density.

the predictions from the theoretical models and global empirical models showing that plumes appear in the duskside as geomagnetic activity increases [*Chappell et al.*, 1970, 1971; *Carpenter et al.*, 1992]. The occurrence rate of the ionospheric outflow (red) events in the duskside (18 events) is slightly higher than that in the dawnside (14 events), indicating that the ionospheric outflow events have a weak dawn-dusk asymmetry.

There is also a clear spatial asymmetry for plumes between Northern and Southern Hemispheres due to the asymmetry of the Cluster orbits between the two hemispheres. For each orbit, there are two magnetopause crossings. The one in the Northern Hemisphere is close to the equator, but the one in the Southern Hemisphere is at high latitudes ($< -10\,R_E$) and near the cusp and mantle region. Therefore, the chances to find the plasmaspheric plume events are higher in the Northern Hemisphere than in the Southern Hemisphere, even though Cluster spent more time in the Southern Hemisphere.

### 3.2. Density Differences

Densities of plumes and ionospheric outflows vary depending on where they were detected and on the geomagnetic activity or solar wind/IMF conditions. Here we focus on the cold ion observations near the magnetopause and compare ion and electron densities of plumes and ionospheric outflows. Figure 4 shows bar plots of the electron density (Figure 4a) obtained through the spacecraft potential measurements from the EFW experiment on Cluster and the ion density (Figure 4b) from the CIS/HIA ion spectrometer for plumes (blue) and ionospheric outflows (red). We used the formula for 2001 observations from *Pedersen et al.* [2008] for a statistical study of the electron density. The densities were averaged over the time period where the low-energy ions were observed. The bin size for all bars is 0.5 cm$^{-3}$.

The median values of the electron density for plume and ionospheric outflow events are 5.4 cm$^{-3}$ and 5.2 cm$^{-3}$, respectively. This indicates that there is no clear difference between the electron density for plumes and for ionospheric outflows. The ion density distributions of both plumes and ionospheric outflows peak at the density range from 0.5 to 1.0 cm$^{-3}$, and the plume ion density distribution only occasionally reaches the density range of 7 to 7.5 cm$^{-3}$. The median ion densities of plumes and ionospheric outflows are 0.9 cm$^{-3}$

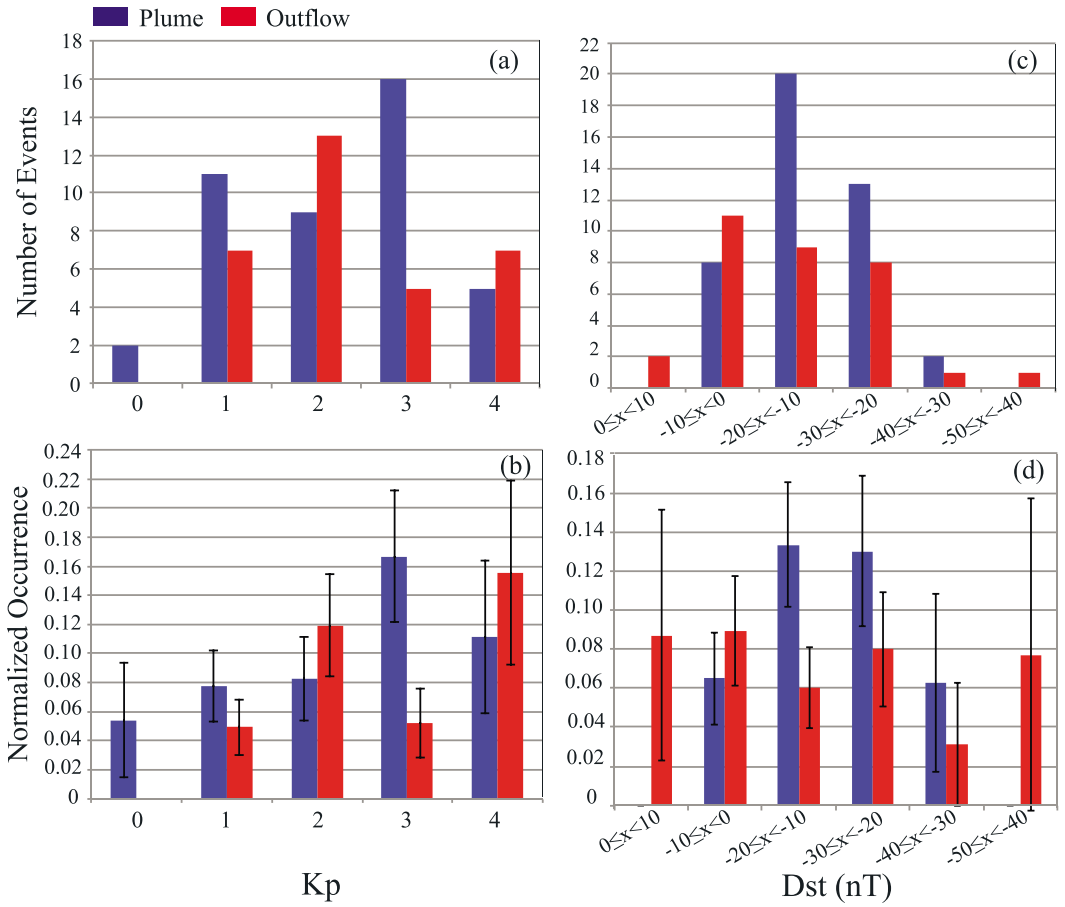


**Figure 5.** Distributions of plume (blue) and ionospheric outflow (red) events as a function of (a) maximum *Kp* in the previous 12 h and (c) minimum *Dst* in the previous 24 h. The normalized occurrence rates of plumes (blue) and ionospheric outflows (red) as a function of (b) *Kp* and (d) *Dst*.

and 0.7 $cm^{-3}$, respectively. The electron densities are higher than the ion densities because the cold ions with energy lower than the threshold (5 eV) of CIS/HIA instrument cannot be detected. Our results show that plasmaspheric plumes are similar to the ionospheric outflows in terms of median ion and electron densities, indicating that number density profile cannot be used to distinguish two different populations near the dayside magnetopause.

### 3.3. Dependence on Geomagnetic Activity

We also examine the relationship between the low-energy ions of two different origins and geomagnetic disturbances. Figure 5 shows the occurrence rates of plumes and ionospheric outflows and their corresponding geomagnetic activity as indicated by the 3 h *K* planetary (*Kp*) index (a and b) and the hourly disturbed storm time (*Dst*) index (c and d). The *Kp* index is expressed as an integer (0, 1, 2, 3, etc.), and each of index value contains a scale of thirds (0, 0+, 1−, 1. 1+, 2−, 2, 2+, etc.). We define the *Kp* values from 0 to 3 as quiet or moderately active magnetospheric conditions, and values greater than 4 as disturbed conditions. *Dst* values greater than 0 correspond to geomagnetically quiet periods, values between 0 and −20 nT to moderate periods, and values below −20 nT to disturbed periods [*Li et al.*, 2012]. We select the maximum *Kp* from the previous 12 h and the minimum *Dst* value from the previous 24 h to account for the response time of the plasmapause to geomagnetic activity [*Moldwin et al.*, 2002, 2004; *Darrouzet et al.*, 2008].

Figures 5a and 5c show the distributions of plumes (blue) and ionospheric outflows (red) as a function of *Kp* and *Dst*, respectively. Figures 5b and 5d show the normalized distributions of plumes (blue) and ionospheric outflows (red) versus *Kp* and *Dst*, respectively. We note that no plumes or ionospheric outflows were observed for the highest *Kp* (>4) and the lowest *Dst* (<−50 nT). The normalized distributions show that the plume events preferentially occur during moderate geomagnetic activity ($Kp = 3$ and $-30\ nT \leq Dst < -10\ nT$).

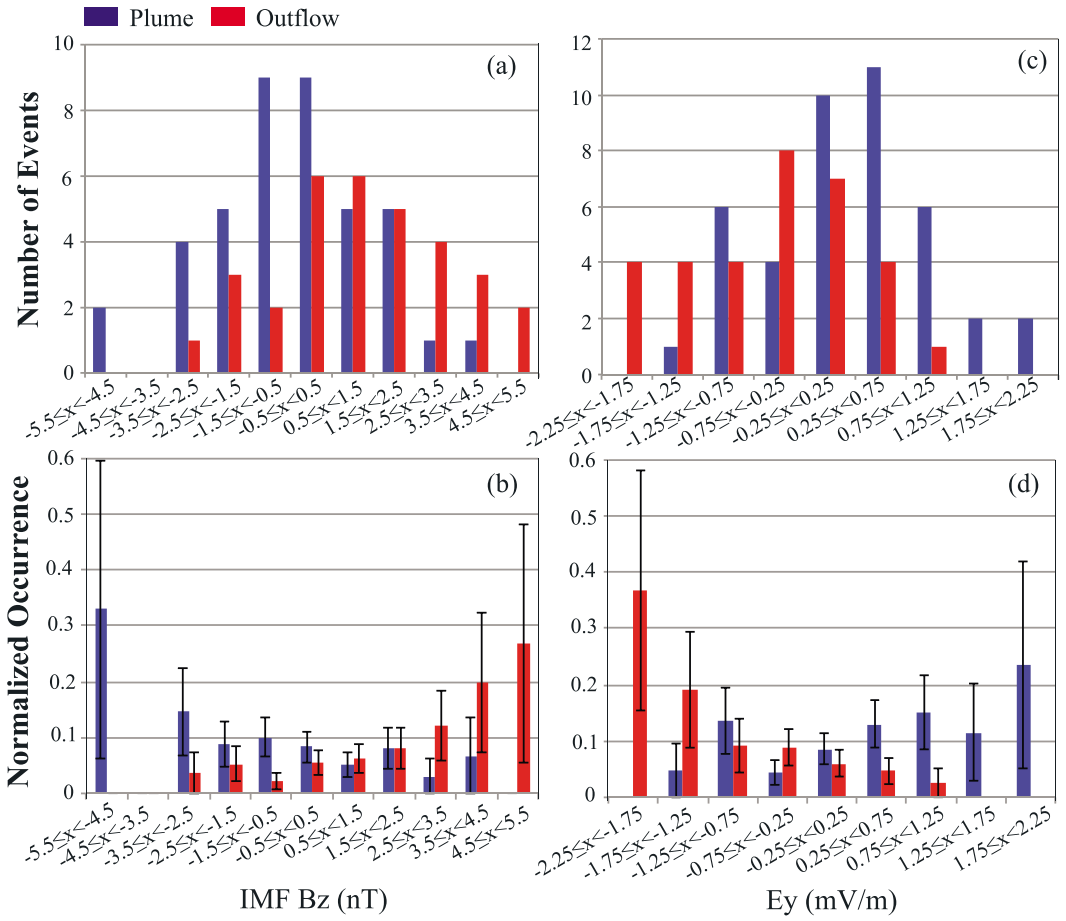


**Figure 6.** Distributions of plumes (blue) and ionospheric outflows (red) as a functions of (a) IMF $B_z$ and (c) $E_y$. Normalized occurrence rates of plume (blue) and ionospheric outflow (red) events as a function of (b) IMF $B_z$ and (d) $E_y$.

The ionospheric outflow events do not occur when $Kp = 0$, and the occurrence rate of the ionospheric outflows does not have a clear *Dst* dependence.

### 3.4. Dependence on Solar Wind Parameters

To investigate the dependence of the occurrence rates of plumes and ionospheric outflows on different solar wind parameters, we use the 5 min averaged multispacecraft OMNIweb data for the selected time period. The OMNIWeb (http://omniweb.gsfc.nasa.gov) combines data from multiple spacecraft (Wind, Geotail, IMP, and ACE) to provide a high-resolution database of IMF and solar wind conditions. The OMNI data sets are time shifted to account for the solar wind propagation time from the spacecraft to the Earth's bow shock. Figures 6a and 6c show the distributions of plasmaspheric plumes (blue) and ionospheric outflows (red) as a function of IMF $B_z$ and the derived solar wind electric field, $E_y$, respectively. The normalized occurrence rates of plumes (blue) and ionospheric outflows (red) as a function of IMF $B_z$ and $E_y$ are shown in Figures 6b and 6d, respectively.

The normalized occurrence rate of plumes increases slowly as values of IMF $B_z$ become more negative, whereas the normalized occurrence rate for ionospheric outflow events tends to increase as the positive IMF $B_z$ values increase (Figure 6b). Thus, the normalized occurrence rates of plumes and ionospheric outflows increase as positive and negative values of $E_y$ increase, respectively (Figure 6d). These observations indicate that the plume events tend to occur during southward IMF (duskward solar wind electric field), whereas the ionospheric outflow events prefer to occur during northward IMF (dawnward solar wind electric field).

Figure 7 shows the distribution of plumes (blue) and ionospheric outflows (red) when (a) IMF $B_y < 0$ and (b) IMF $B_y > 0$ in the GSM *X*-*Y* plane. About 65% of the low-energy ion events (both plume and ionospheric outflow) were observed during positive IMF $B_y$, while only 35% were observed during negative IMF $B_y$. Notably,

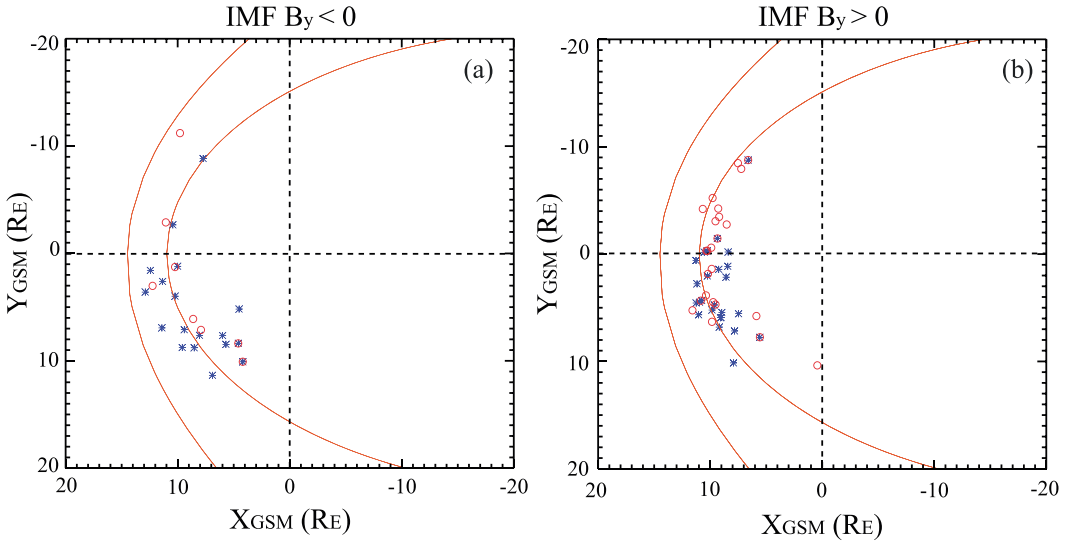


**Figure 7.** Distributions of plumes (blue) and ionospheric outflows (red) when the (a) IMF $B_y < 0$ and (b) IMF $B_y > 0$ in the *X*-*Y* GSM plane.

significantly more ionospheric outflows (red) were observed during positive IMF $B_y$ (24 of 32, 75%) than during negative IMF $B_y$ (8 of 32, 25%).

Seventy-five percent of the ionospheric outflows were observed in the duskside for negative IMF $B_y$, while 46% of the ionospheric outflows were observed in the duskside for positive IMF $B_y$. Fifty-four percent of the ionospheric outflows were observed in the dawnside when IMF $B_y$ was positive, while 25% of the ionospheric outflows were observed in the dawnside when the IMF $B_y$ was negative. These results show the effect of IMF $B_y$ on the occurrence rate of ionospheric outflows. This is consistent with the results from *Chen and Moore* [2006], who showed that the occurrence rate of the low-energy ion events on the dawnside increases when the IMF $B_y$ is positive. In contrast to the occurrence rate of ionospheric outflows, more plume events were found at the duskside whether IMF $B_y > 0$ or IMF $B_y < 0$. The occurrence rate of plumes in the duskside (39 of 43, 91%) is much higher than that in the dawnside (9%).

Figure 8a shows the distributions of plumes (blue) and ionospheric outflows (red) as a function of the solar wind dynamic pressure obtained from OMNIweb. A majority of plumes and ionospheric outflows occurs when the solar wind dynamic pressure is between 1 and 2 nPa. The normalized occurrence rates of both plumes (blue) and ionospheric outflows (red) increase with the solar wind dynamic pressure (Figure 8b).

## 4. Discussion

### 4.1. Geomagnetic Activity Effects on the Occurrence Rate for Plumes and Ionospheric Outflows

Geomagnetic activity is one of the driving mechanisms for the generation of plasmaspheric plumes. During periods of higher geomagnetic activity, the plasmasphere shrinks in size due to strong sunward convection and the plasmaspheric particles that were originally located in the outermost closed drift region suddenly find themselves on open convection paths and can reach the dayside magnetopause. *Darrouzet et al.* [2008] showed that more plasmaspheric plume events were observed during moderate activity (*Kp* between 3+ and 6) between 1 February 2001 and 1 February 2006.

Ions in the ionosphere can escape when their velocities reach the escape velocity via several energization mechanisms such as centrifugal acceleration, wave heating, ambipolar electric field, and joule heating. For example, electron heating induces the enhanced ambipolar electric field that produces ionospheric outflows. It acts against the gravitational force and reduces the escape velocity. The escape of ionospheric heavy ions depends on both the solar electromagnetic and solar wind energy inputs [*Yau et al.*, 1984]. *Yau et al.* [1984] and *Abe et al.* [1996] found that the ionospheric outflow rate of $H^+$ and $O^+$ ions and the occurrence rate of both species depend weakly on the magnetic activity (*Kp* index). *Li et al.* [2012], however, showed that the elevated ionospheric outflow fluxes were observed near the dayside cusp region and the nightside auroral

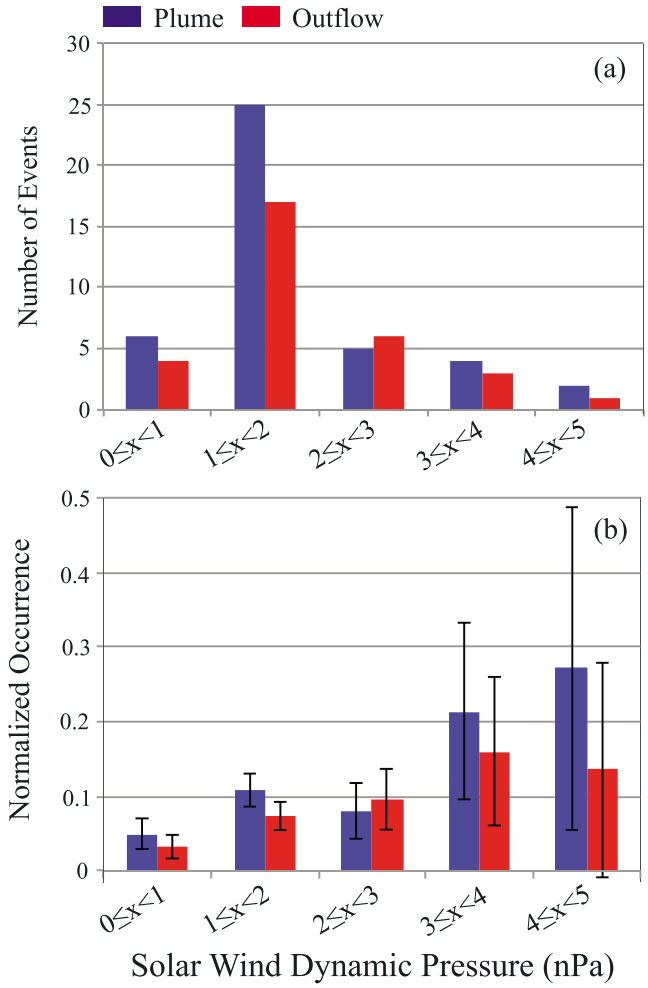


**Figure 8.** (a) Distributions of plumes (blue) and ionospheric outflows (red) as a function of the solar wind dynamic pressure and (b) the normalized occurrence rates of plumes (blue) and ionospheric outflows (red) as a function of the solar wind dynamic pressure.

region during disturbed magnetospheric conditions ($Dst < -20$ nT). This difference may be caused by the different locations where the low-energy ions were observed.

### 4.2. IMF $B_z$ Effects on the Occurrence Rates of Plasmaspheric Plumes and Ionospheric Outflows

Sixty-seven percent (29 of 43) of the plume events were observed during southward IMF, while only 33% were observed during northward IMF. Significantly more plume events were observed in the duskside (91%, 39 of 43) than in the dawnside (See Figure 7).

The occurrence rate of plasmaspheric plumes is strongly correlated with high geomagnetic activity as well as intervals of southward IMF [*Horwitz et al.*, 1990; *Carpenter et al.*, 1993; *Moldwin et al.*, 2003; *Goldstein et al.*, 2003]. For southward IMF, dayside magnetopause reconnection occurs and primarily drives antisunward flow in the ionospheric polar cap, with a return sunward convection at lower latitudes [*Dungey*, 1961; *Heppner*, 1972]. This sunward convection in the inner magnetosphere causes the erosion of the outer portion of the rotating plasmasphere. The plasmaspheric drainage plume can be formed during intervals of enhanced magnetospheric convection. Many observations [*Chappell*, 1972; *Chen and Moore*, 2006; *Kim et al.*, 2007; *Darrouzet et al.*, 2008; *Walsh et al.*, 2013] have shown that plumes are more often found in the duskside than in the dawnside, which is consistent with the dawn-dusk asymmetry of the occurrence rate of plumes presented in this paper.

The higher occurrence rate of the ionospheric outflow was observed for the northward IMF (IMF $B_z > 0$, dawnward solar wind electric field) (Figures 6b and 6d). *Ridley et al.* [1998] have shown that the changes of the IMF orientation determine the shape of the ionospheric electric potential pattern. For northward IMF,

the ionospheric convection pattern is more complicated than that for southward IMF. For strongly northward IMF, the two-cell convection pattern forms in the high-latitude ionosphere with a counterclockwise duskside cell and a clockwise dawnside cell. This pattern indicates that the magnetic flux is being convected from the tail to the dayside (sunward flowing) in the high-latitude ionosphere [*Reiff and Burch*, 1985; *Ridley et al.*, 1998]. The ionospheric outflow can be convected toward dayside along with the magnetic flux. Thus, the occurrence rate of the ionospheric outflows observed at the dayside magnetopause increases when the IMF is strongly northward.

### 4.3. IMF $B_y$ Effects on the Occurrence Rate of the Ionospheric Outflows

The effects of IMF $B_y$ on the dawn-dusk asymmetry of the convection pattern, auroral oval, and electric field in the ionosphere have been studied [*Mozer and Lucht*, 1974; *Raitt et al.*, 1977; *Holzworth and Meng*, 1984; *Reiff and Burch*, 1985; *Lu et al.*, 1989; *Cowley et al.*, 1991].

The two convection cells in the high-latitude ionosphere are symmetric for strongly northward IMF with negligible IMF $B_y$ [*Reiff and Burch*, 1985; *Ridley et al.*, 1998]. In the presence of IMF $B_y$, these two convection cells become asymmetric. For positive (negative) IMF $B_y$, both convection cells are clockwise (counterclockwise) and the dawnside (duskside) cell is larger than the duskside (dawnside) cell in the Northern Hemisphere [*Reiff and Burch*, 1985]. These convection patterns indicate that the plasma flows sunward at the dawnside (duskside) in the high-latitude ionosphere during strongly northward IMF with a positive (negative) IMF $B_y$ component.

The auroral oval is shifted toward dawn in the Northern Hemisphere for positive IMF $B_y$ and toward dusk for negative IMF $B_y$ [*Holzworth and Meng*, 1984]. As the auroral zone is one of the source regions of the ionospheric outflow, the shift toward dawnside for positive IMF $B_y$ can lead to a higher occurrence rate of the ionospheric outflows at the dawnside.

The dawn-dusk asymmetry of the electric field in the ionosphere is related to the sign and magnitude of IMF $B_y$. The electric field near local dawn in the Northern Hemisphere is enhanced when the IMF $B_y > 0$, whereas the electric field near local dusk is increased in the Northern Hemisphere when the IMF $B_y < 0$ [*Mozer and Lucht*, 1974]. This convection electric field can significantly increase the proton temperature and cause a high outward flux of protons for average ionospheric conditions at high altitudes [*Raitt et al.*, 1977].

Changes in the convection cell patterns, the auroral oval, and the electric field in the ionosphere predict enhanced ionospheric outflows in the dawnside during positive IMF $B_y$ and in the duskside during negative IMF $B_y$ in the Northern Hemisphere. The dawn-dusk asymmetries in the Southern Hemisphere are in the opposite sense to the asymmetries in the Northern Hemisphere [*Mozer and Lucht*, 1974; *Raitt et al.*, 1977; *Cowley et al.*, 1991]. Cluster observations of outflows occur near the equator, and the outflows most likely originate in both the northern and southern ionospheres. If the contribution from the two hemispheres are equal and if the dawn-dusk asymmetry in both hemispheres are similar, then no IMF $B_y$ effect on the occurrence rate of ionospheric outflows is expected from Cluster observations. However, the dawn-dusk asymmetry is different in the two hemispheres. *Lu et al.* [1989] found that the dawn-dusk asymmetry in the Southern Hemisphere is weaker than that in the Northern Hemisphere using the distributions of the convection potential around the polar cap boundary measured by AE-C, AE-D, and DE2. Therefore, more outflow events were expected to be observed in the dawnside during positive IMF $B_y$ and in the duskside during negative IMF $B_y$. Indeed, 75% of ionospheric outflow events were observed in the duskside for negative IMF $B_y$. On the other hand, 54% of outflow events were observed in the dawnside for positive IMF $B_y$.

### 4.4. Solar Wind Dynamic Pressure Effects on the Occurrence Rates of Plasmaspheric Plumes and Ionospheric Outflows

The occurrence rates of plasmaspheric plumes and ionospheric outflows were strongly correlated with the solar wind dynamic pressure (Figure 8b). Strong magnetospheric compression causes the dayside magnetopause to move inward so that the plasmaspheric ions can be observed near the compressed magnetopause [*Elphic et al.*, 1996; *Kim et al.*, 2007]. *Kim et al.* [2007] reported that cold dense plasmaspheric plasma was observed by Polar, which crossed the magnetopause at $L = \sim 5.5-6.0$ when the solar wind dynamic pressure was high and the IMF was strongly southward.

Many observational studies have shown that peak upwelling flux and occurrence rate of the ionospheric upwelling ions are correlated with solar dynamic pressure, which is one of the driving parameters

[*Giles*, 1993; *Moore et al.*, 1999; *Elliott et al.*, 2001; *Echer et al.*, 2008]. The solar wind dynamic pressure drives strong ionospheric bulk heating that causes the ionospheric ions to escape from the ionosphere.

## 5. Summary and Conclusions

We presented a statistical study of plasmaspheric plumes and ionospheric outflows observed by C3 near the dayside magnetopause between 2007 and 2009. We identified 43 plume events with perpendicular pitch angle distributions and 32 ionospheric outflow events with unidirectional or bidirectional field-aligned pitch angle distributions during 442 dayside magnetopause crossings. The characteristics between plumes and ionospheric outflows were compared, and we also investigated the relation between the occurrence rates of the plume and ionospheric outflow events and their locations, and their dependence on geomagnetic activity and solar wind/IMF conditions. The main results of this paper can be summarized as follows:

1. The occurrence rate of plumes is significantly higher in the duskside than that in the dawnside. However, the occurrence rate of ionospheric outflows shows a weak dawn-dusk asymmetry.
2. The median values of the electron (ion) density of plumes and ionospheric outflows are 5.4 $cm^{-3}$ and 5.2 $cm^{-3}$ (0.9 $cm^{-3}$ and 0.7 $cm^{-3}$), respectively.
3. Plasmaspheric plumes prefer to occur during moderate conditions ($Kp = 3$ and $-30 \leq Dst < -10$ nT). Ionospheric outflows do not occur when $Kp = 0$ and the occurrence rate of ionospheric outflows does not have clear *Dst* dependence.
4. The plume events tend to occur during southward IMF (duskward solar wind electric field), whereas the ionospheric outflow events tend to occur during northward IMF (dawnward solar wind electric field).
5. Enhanced occurrence rates of ionospheric outflows were observed in the dawnside (duskside) when IMF $B_y > 0$ (IMF $B_y < 0$).
6. The occurrence rates of both plumes and ionospheric outflows increase as the solar wind dynamic pressure increases.

**Acknowledgments**
We thank the instrument teams of Cluster mission and ESA Cluster Science Archive for the successful spacecraft operation and for providing plasma and magnetic field data (http://www.cosmos.esa.int/web/csa). The *Kp* and *Dst* indices were provided by the website (http://wdc.kugi.kyoto-u.ac.jp/). The IMF and the derived solar wind electric field, $E_y$, were provided by the OMNIWeb (http://omniweb.gsfc.nasa.gov/). H. Zhang was supported by NSF grant AGS-1007449. Q.-G. Zong was supported by National Natural Science Foundation of China (41421003) and Major Project of Chinese National Programs for Fundamental Research and Development (2012CB825603). E. Liebert was financially supported through grant 50 OC1402 by the Deutsches Zentrum für Luft- und Raumfahrt.

## References

Abe, T., S. Watanabe, B. A. Whalen, A. W. Yau, and E. Sagawa (1996), Observations of polar wind and thermal ion outflow by Akebono/SMS, *J. Geomagn. Geoelectr.*, *48*(3), 319–325, doi:10.5636/jgg.48.319.

Andersson, L., W. K. Peterson, and K. M. McBryde (2005), Estimates of the suprathermal $O^+$ outflow characteristic energy and relative location in the auroral oval, *Geophys. Res. Lett.*, *32*, L09104, doi:10.1029/2004GL021434.

André, M., and C. M. Cully (2012), Low-energy ions: A previously hidden solar system particle population, *Geophys. Res. Lett.*, *39*, L03101, doi:10.1029/2011GL050242.

Balogh, A., et al. (2001), The Cluster magnetic field investigation: Overview of in-flight performance and initial results, *Ann. Geophys.*, *19*, 1207–1217, doi:10.5194/angeo-19-1207-2001.

Baugher, C. R., C. R. Chappell, J. L. Horwitz, E. G. Shelley, and D. T. Young (1980), Initial thermal plasma observations from ISEE-1, *Geophys. Res. Lett.*, *7*, 657–660, doi:10.1029/GL007i009p00657.

Borovsky, J. E., M. Hesse, J. Birn, and M. M. Kuznetsova (2008), What determines the reconnection rate at the dayside magnetosphere?, *J. Geophys. Res.*, *113*, A07210, doi:10.1029/2007JA012645.

Borovsky, J. E., M. H. Denton, R. E. Denton, V. K. Jordanova, and J. Krall (2013), Estimating the effects of ionospheric plasma on solar wind/magnetosphere coupling via mass loading of dayside reconnection: Ion-plasma-sheet oxygen, plasmaspheric drainage plumes, and the plasma cloak, *J. Geophys. Res. Space Physics*, *118*, 5695–5719, doi:10.1002/jgra.50527.

Carpenter, D. L., A. J. Smith, B. L. Giles, C. R. Chappell, and P. M. E. Décréau (1992), A case study of plasma structure in the dusk sector associated with enhanced magnetospheric convection, *J. Geophys. Res.*, *97*, 1157–1166, doi:10.1029/91JA01546.

Carpenter, D. L., B. L. Giles, C. R. Chappell, P. M. E. Décréau, R. R. Anderson, A. M. Persoon, A. J. Smith, Y. Corcuff, and P. Canu (1993), Plasmasphere dynamics in the duskside bulge region: A new look at old topic, *J. Geophys. Res.*, *98*, 19,243–19,271, doi:10.1029/93JA00922.

Chappell, C. R. (1972), Recent satellite measurements of the morphology and dynamics of the plasmasphere, *Rev. Geophys.*, *10*, 951–979, doi:10.1029/RG010i004p00951.

Chappell, C. R. (1974), Detached plasma regions in the magnetosphere, *J. Geophys. Res.*, *79*, 1861–1870, doi:10.1029/JA079i013p01861.

Chappell, C. R., K. K. Harris, and G. W. Sharp (1970), The morphology of the bulge region of the plasmasphere, *J. Geophys. Res.*, *75*, 3848–3861, doi:10.1029/JA075i019p03848.

Chappell, C. R., K. K. Harris, and G. W. Sharp (1971), The dayside of the plasmasphere, *J. Geophys. Res.*, *76*, 7632–7647, doi:10.1029/JA076i031p07632.

Chappell, C. R., M. M. Huddleston, T. E. Moore, B. L. Giles, and D. C. Delcourt (2008), Observations of the warm plasma cloak and an explanation of its formation in the magnetosphere, *J. Geophys. Res.*, *113*, A09206, doi:10.1029/2007JA012945.

Chen, A. J., and R. A. Wolf (1972), Effects on the plasmasphere of a time-varying convection electric field, *Planet. Space Sci.*, *20*, 483–509, doi:10.1016/0032-0633(72)90080-3.

Chen, S.-H., and T. E. Moore (2006), Magnetospheric convection and thermal ions in the dayside outer magnetosphere, *J. Geophys. Res.*, *111*, A03215, doi:10.1029/2005JA011084.

Cowley, S. W. H., J. P. Morelli, and M. Lockwood (1991), Dependence of convective flows and particle precipitation in the high-latitude dayside ionosphere on the X and Y components of the interplanetary magnetic field, *J. Geophys. Res.*, *96*, 5557–5564, doi:10.1029/90JA02063.

Cully, C. M., E. F. Donovan, A. W. Yau, and G. G. Arkos (2003), Akebono/suprathermal mass spectrometer observations of low-energy ion outflow: Dependence on magnetic activity and solar wind conditions, *J. Geophys. Res.*, *108*, 1093, doi:10.1029/2001JA009200.

Dandouras, I. (2013), Detection of a plasmaspheric wind in the Earth's magnetosphere by the Cluster spacecraft, *Ann. Geophys.*, *31*, 1143–1153, doi:10.5194/angeo-31-1143-2013.

Darrouzet, F., J. de Keyser, P. M. E. Décréau, F. El Lemdani-Mazouz, and X. Vallières (2008), Statistical analysis of plasmaspheric plumes with Cluster/WHISPER observations, *Ann. Geophys.*, *26*, 2403–2417, doi:10.5194/angeo-26-2403-2008.

Dungey, J. W. (1961), Interplanetary magnetic field and the auroral zones, *Phys. Rev. Lett.*, *6*, 47–48.

Echer, E., A. Korth, Q.-G. Zong, M. Fraünz, W. D. Gonzalez, F. L. Guarnieri, S. Y. Fu, and H. Reme (2008), Cluster observations of $O^+$ escape in the magnetotail due to shock compression effects during the initial phase of the magnetic storm on 17 August 2001, *J. Geophys. Res.*, *113*, A05209, doi:10.1029/2007JA012624.

Elliott, H. A., R. H. Comfort, P. D. Craven, M. O. Chandler, and T. E. Moore (2001), Solar wind influence on the oxygen content of ion outflow in the high-altitude polar cap during solar minimum conditions, *J. Geophys. Res.*, *106*, 6067–6084, doi:10.1029/2000JA003022.

Elphic, R. C., L. A. Weiss, M. F. Thomsen, D. J. McComas, and M. B. Moldwin (1996), Evolution of plasmaspheric ions at geosynchronous orbit during times of high geomagnetic activity, *Geophys. Res. Lett.*, *23*, 2189–2192, doi:10.1029/96GL02085.

Escoubet, C. P., C. T. Russell, and R. Schmidt (1997), *The Cluster and Phoenix Missions*, vol. 79, pp. 1–2, reprinted from Space Sci. Rev. Kluwer Acad., Dordretch, Netherlands.

Escoubet, C. P., M. Fehringer, and M. Goldstein (2001), Introduction: The Cluster mission, *Ann. Geophys.*, *19*, 1197–1200, doi:10.5194/angeo-19-1197-2001.

Fennell, J. F., D. R. Croley Jr., and S. M. Kaye (1981), Low-energy ion pitch angle distributions in the outer magnetosphere—Ion zipper distributions, *J. Geophys. Res.*, *86*, 3375–3382, doi:10.1029/JA086iA05p03375.

Giles, B. L. (1993), *Inner Magnetosphere Circulation of Thermal Ions Inferred From Observed Pitch Angle Distributions, Dissertation Abstracts Intl.*, vol. 54–12, 6264 pp., Univ. of Alabama in HuntsvillE.

Giles, B. L., C. R. Chappell, T. E. Moore, R. H. Comfort, and J. H. Waite Jr. (1994), Statistical survey of pitch angle distributions in core (0–50 eV) ions from Dynamics Explorer 1: Outflow in the auroral zone, polar cap, and cusp, *J. Geophys. Res.*, *99*, 17,483–17501, doi:10.1029/94JA00864.

Goldstein, J., B. R. Sandel, M. R. Hairston, and P. H. Reiff (2003), Control of plasmaspheric dynamics by both convection and sub-auroral polarization stream, *Geophys. Res. Lett.*, *30*, 2243, doi:10.1029/2003GL018390.

Goldstein, J., B. R. Sandel, M. F. Thomsen, M. Spasojević, and P. H. Reiff (2004), Simultaneous remote sensing and in situ observations of plasmaspheric drainage plumes, *J. Geophys. Res.*, *109*, A03202, doi:10.1029/2003JA010281.

Goldstein, J., B. R. Sandel, W. T. Forrester, M. F. Thomsen, and M. R. Hairston (2005), Global plasmasphere evolution 22–23 April 2001, *J. Geophys. Res.*, *110*, A12218, doi:10.1029/2005JA011282.

Green, J. L., B. R. Sandel, S. F. Fung, D. L. Gallagher, and B. W. Reinisch (2002), On the origin of kilometric continuum, *J. Geophys. Res.*, *107*, 1105, doi:10.1029/2001JA000193.

Gustafsson, G., et al. (2001), First results of electric field and density observations by CLUSTER EFW based on initial months of operation, *Ann. Geophys.*, *19*, 1219–1240.

Heppner, J. P. (1972), Polar-cap electric field distributions related to the interplanetary magnetic field direction, *J. Geophys. Res.*, *77*, 4877–4887, doi:10.1029/JA077i025p04877.

Holzworth, R. H., and C.-I. Meng (1984), Auroral boundary variations and the interplanetary magnetic field, *Planet. Space Sci.*, *32*, 25–29, doi:10.1016/0032-0633(84)90038-2.

Horwitz, J. L., C. R. Baugher, C. R. Chappell, E. G. Shelley, and D. T. Young (1982), Conical pitch angle distributions of very low-energy ion fluxes observed by ISEE 1, *J. Geophys. Res.*, *87*, 2311–2320, doi:10.1029/JA087iA04p02311.

Horwitz, J. L., R. H. Comfort, and C. R. Chappell (1990), A statistical characterization of plasmasphere density structure and boundary locations, *J. Geophys. Res.*, *95*, 7937–7947, doi:10.1029/JA095iA06p07937.

Kaye, S. M., E. G. Shelley, R. D. Sharp, and R. G. Johnson (1981), Ion composition of zipper events, *J. Geophys. Res.*, *86*, 3383–3388, doi:10.1029/JA086iA05p03383.

Kim, K.-H., J. Goldstein, and D. Berube (2007), Plasmaspheric drainage plume observed by the Polar satellite in the prenoon sector and the IMAGE satellite during the magnetic storm of 11 April 2001, *J. Geophys. Res.*, *112*, A06237, doi:10.1029/2006JA012030.

Lee, S. H., H. Zhang, Q.-G. Zong, A. Otto, D. G. Sibeck, Y. Wang, K.-H. Glassmeier, P. W. Daly, and H. Rème (2014), Plasma and energetic particle behaviors during asymmetric magnetic reconnection at the magnetopause, *J. Geophys. Res.*, *119*, 1658–1672, doi:10.1002/2013JA019168.

Lemaire, J. (2000), The formation plasmaspheric tails, *Phys. Chem. Earth*, *25*, 9–17, doi:10.1016/S1464-1917(99)00026-4.

Lennartsson, W., and D. L. Reasoner (1978), Low-energy plasma observations at synchronous orbit, *J. Geophys. Res.*, *83*, 2145–2156, doi:10.1029/JA083iA05p02145.

Li, K., et al. (2012), On the ionospheric source region of cold ion outflow, *Geophys. Res. Lett.*, *39*, L18102, doi:10.1029/2012GL053297.

Lu, G., P. H. Reiff, J. L. Karty, M. R. Hairston, and R. A. Heelis (1989), Distribution of convection potential around the polar cap boundary as a function of the interplanetary magnetic field, *J. Geophys. Res.*, *94*, 13,447–13,461, doi:10.1029/JA094iA10p13447.

Moldwin, M. B., L. Downward, H. K. Rassoul, R. Amin, and R. R. Anderson (2002), A new model of the location of the plasmapause: CRRES results, *J. Geophys. Res.*, *107*(A11), 1339, doi:10.1029/2001JA009211.

Moldwin, M. B., B. R. Sandel, M. F. Thomsen, and R. C. Elphic (2003), Quantifying global plasmaspheric images with in situ observations, *Space Sci. Rev.*, *109*, 47–61, doi:10.1023/B:SPAC.0000007512.69979.8f.

Moldwin, M. B., J. Howard, J. Sanny, J. D. Bocchicchio, H. K. Rassoul, and R. R. Anderson (2004), Plasmaspheric plumes: CRRES observations of enhanced density beyond the plasmapause, *J. Geophys. Res.*, *109*, A05202, doi:10.1029/2003JA010320.

Moore, T. E., et al. (1999), Ionospheric mass ejection in response to a CME, *Geophys. Res. Lett.*, *26*, 2339–2342, doi:10.1029/1999GL900456.

Mozer, F. S., and P. Lucht (1974), The average auroral zone electric field, *J. Geophys. Res.*, *79*, 1001–1006, doi:10.1029/JA079i007p01001.

Murakami, G., I. Yoshikawa, K. Yoshioka, A. Yamazaki, M. Kagitani, M. Taguchi, M. Kikuchi, S. Kameda, and M. Nakamura (2013), Plasmaspheric filament: An isolated magnetic flux tube filled with dense plasmas, *Geophys. Res. Lett.*, *40*, 250–254, doi:10.1002/grl.50124.

Nagai, T., J. F. E. Johnson, and C. R. Chappell (1983), Low-energy (<100 eV) ion pitch angle distributions in the magnetosphere by ISEE 1, *J. Geophys. Res.*, *88*, 6944–6960, doi:10.1029/JA088iA09p06944.

O'Brien, T. P., and M. B. Moldwin (2003), Empirical plasmapause models from magnetic indices, *Geophys. Res. Lett.*, *30*, 1152, doi:10.1029/2002GL016007.

Pedersen, A., et al. (2008), Electron density estimations derived from spacecraft potential measurements on Cluster in tenuous plasma regions, *J. Geophys. Res.*, *113*, A07S33, doi:10.1029/2007JA012636.

Peterson, W. K., H. L. Collin, A. W. Yau, and O. W. Lennartsson (2001), Polar/Toroidal Imaging Mass-Angle Spectrograph observations of suprathermal ion outflow during solar minimum conditions, *J. Geophys. Res.*, *106*, 6059–6066, doi:10.1029/2000JA003006.

Peterson, W. K., H. L. Collin, O. W. Lennartsson, and A. W. Yau (2006), Quiet time solar illumination effects on the fluxes and characteristic energies of ionospheric outflow, *J. Geophys. Res.*, *111*, A11S05, doi:10.1029/2005JA011596.

Raitt, W. J., R. W. Schunk, and P. M. Banks (1977), The influence of convection electric fields on thermal proton outflow from the ionosphere, *Planet. Space Sci.*, *25*, 291–301, doi:10.1016/0032-0633(77)90139-8.

Redmon, R. J., W. K. Peterson, L. Andersson, and P. G. Richards (2012), Dawnward shift of the dayside $O^+$ outflow distribution: The importance of field line history in $O^+$ escape from the ionosphere, *J. Geophys. Res.*, *117*, A12222, doi:10.1029/2012JA018145.

Reiff, P. H., and J. L. Burch (1985), IMF by-dependent plasma flow and Birkeland currents in the dayside magnetosphere: 2. A global model for northward and southward IMF, *J. Geophys. Res.*, *90*(A2), 1595–1609, doi:10.1029/JA090iA02p01595.

Rème, H., et al. (2001), First multispacecraft ion measurements in and near the Earth's magnetosphere with the identical Cluster Ion Spectrometry (CIS) experiment, *Ann. Geophys.*, *19*, 1303–1354.

Ridley, A. J., G. Lu, C. R. Clauer, and V. O. Papitashvili (1998), A statistical study of the ionospheric convection response to changing interplanetary magnetic field conditions using the assimilative mapping of ionospheric electrodynamics technique, *J. Geophys. Res.*, *103*, 4023–4040, doi:10.1029/97JA03328.

Sagawa, E., A. W. Yau, B. A. Whalen, and W. K. Peterson (1987), Pitch angle distributions of low-energy ions in the near-Earth magnetosphere, *J. Geophys. Res.*, *92*, 12,241–12,254, doi:10.1029/JA092iA11p12241.

Sauvaud, J.-A., et al. (2001), Intermittent thermal plasma acceleration linked to sporadic motions of the magnetopause, first Cluster results, *Ann. Geophys.*, *19*, 1523, doi:10.5194/angeo-19-1523-2001.

Shay, M. A., and M. Swisdak (2004), Three-species collisionless reconnection: Effect of $O^+$ on magnetotail reconnection, *Phys. Rev. Lett.*, *93*(17), 175001, doi:10.1103/PhysRevLett.93.175001.

Sheeley, B. W., M. B. Moldwin, H. K. Rassoul, and R. R. Anderson (2001), An empirical plasmasphere and trough density model: CRRES observations, *J. Geophys. Res.*, *106*, 25,631–25,642, doi:10.1029/2000JA000286.

Walsh, B. M., D. G. Sibeck, Y. Nishimura, and V. Angelopoulos (2013), Statistical analysis of the plasmaspheric plume at the magnetopause, *J. Geophys. Res. Space Physics*, *118*, 4844–4851, doi:10.1002/jgra.50458.

Wang, S., L. M. Kistler, C. G. Mouikis, Y. Liu, and K. J. Genestreti (2014), Hot magnetospheric $O^+$ and cold ion behavior in magnetopause reconnection: Cluster observations, *J. Geophys. Res.*, *119*, 9601–9623, doi:10.1002/2014JA020402.

Yau, A. W., and M. André (1997), Sources of ion outflow in the high latitude ionosphere, *Space Sci. Rev.*, *80*, 1–25.

Yau, A. W., B. A. Whalen, W. K. Peterson, and E. G. Shelley (1984), Distribution of upflowing ionospheric ions in the high-altitude polar cap and auroral ionosphere, *J. Geophys. Res.*, *89*, 5507–5522.

Yau, A. W., E. G. Shelley, and W. K. Peterson (1986), Accelerated auroral and polar-cap ions: Outflow at DE-1 altitudes, in *Ion Acceleration in the Magnetosphere and Ionosphere*, vol. 38, edited by T. Chang et al., pp. 72–76, AGU, doi:10.1029/GM038p0072.

Yau, A. W., T. Abe, and W. K. Peterson (2007), The polar wind: Recent observations, *J. Atmos. Terr. Phys.*, *69*, 1936–1983, doi:10.1016/j.jastp.2007.08.010.